

Low-Thrust Aldrin Cyclers with Reduced Encounter Velocities

K. Joseph Chen,¹ Masataka Okutsu,² Damon F. Landau,² and
James M. Longuski³

*School of Aeronautics and Astronautics, Purdue University
West Lafayette, Indiana 47907-2023*

We design a new version of a cycler orbit between Earth and Mars (known as the Aldrin cycler) in which we use low thrust to reduce the encounter velocities. We show that by reducing the encounter velocities at both planets, the propellant needed by the taxis to perform hyperbolic rendezvous can be significantly reduced. If the V-infinity reduction is large enough, two-stage taxis can be used instead of three-stage taxis, thus further reducing the required injected mass to a low-Earth orbit (IMLEO) for a particular cycler trajectory. However, as the V-infinity decreases, the propellant expenditure for the cycler vehicle increases. Our trade studies (over seven synodic periods) show that V-infinity reductions can be effective in reducing the total IMLEO (i.e. cycler plus taxi) propellant for low-thrust Aldrin cycler missions.

I. Introduction

NUMEROUS ways of transporting humans from Earth to Mars (and back to Earth) have been analyzed over the years.¹⁻¹⁰ The simplest architecture is to directly launch from the Earth to Mars, land, and then repeat the process to come back to Earth. In this (“Direct”) case a separate set of hardware and consumables is needed for each launch. Alternatives to direct launches are cycling trajectories. A common feature of all cyclers is the reuse of the cycling spacecraft, thus eliminating the need to re-launch most of the hardware. These cycling trajectories (or cyclers) have been discovered and studied since the 1960s.²⁻⁸ The most well-known among these cyclers is the Aldrin cycler.⁵⁻⁶

The Aldrin cycler comprises two mirroring trajectories. These are called the outbound cycler (or sometimes the “up escalator”) and the inbound cycler (or the “down escalator”).⁵⁻⁶ The outbound cycler provides short (typically 6-month) trips from Earth to Mars, but take much longer (about 1.6 years) to return from Mars to Earth. The inbound cycler is the mirror image of the outbound, providing short return trips from Mars to Earth but having longer Earth-Mars transits. An architecture that uses the Aldrin cycler to transport people would take advantage of the short transfers of the inbound and outbound cyclers to reduce travel time between Earth and Mars.⁹⁻¹⁰ At each flyby, smaller spacecraft called “taxis” would ferry astronauts between the spacecraft on the cycler trajectory (hereafter “cycler vehicle”) and the surfaces of the planets. The taxis then perform hyperbolic¹¹ rendezvous with the cycler vehicles to safely complete the transfer of humans.

Unfortunately the hyperbolic rendezvous sometimes have very high V_∞ at Mars (ranging from about 6 km/s to over 12 km/s). These high V_∞ make the hyperbolic rendezvous costly in terms of taxi propellant, especially at Mars.⁹⁻¹⁰ The rendezvous are more manageable at Earth for two main reasons: first, the V_∞ are lower (5 to 7 km/s), and second, the propellant is more easily obtained at Earth. In this paper, we design a modified low-thrust version of the Aldrin cycler with lower V_∞ at Mars. We expect to see a significant reduction in the taxi propellant usage, while accruing a moderate increase in the propellant used by the

¹ Doctoral Candidate, School of Aeronautics and Astronautics, 315 N. Grant St.

² Doctoral Candidate, School of Aeronautics and Astronautics, 315 N. Grant St, Student Member AIAA, Member AAS.

³ Professor, Associate Fellow AIAA, School of Aeronautics and Astronautics, 315 N. Grant St Member AAS.

cycler vehicles. We perform trade studies to show that this propellant trade leads to lower total IMLEO cost to maintain the cycling transportation system.

II. Methodology

We use a low-thrust trajectory optimizer developed at Purdue University (based on earlier work by Sims and Flanagan¹² called GALLOP. GALLOP stands for Gravity-Assist, Low-thrust Local Optimization Program.¹³⁻¹⁶ GALLOP transforms the trajectory optimization problem into a nonlinear programming (NLP) problem and maximizes the final spacecraft mass; it is driven by a sequential quadratic programming algorithm, SNOPT.¹⁷

The trajectory model in GALLOP divides each planet-planet leg of the trajectory into segments of equal duration. The thrusting on each segment is modeled by an impulse at the midpoint of the segment, with conic arcs between the impulses. Each leg is propagated half-way forward from the initial body and half-way backward from the final body. In order to have a feasible trajectory, one of the constraints that must be satisfied is that the forward- and backward-propagated half-legs must meet at a match-point in the middle of the leg. The planetary positions and velocities are determined using an integrated (or analytic) ephemeris such as the Jet Propulsion Laboratory's DE405.

The optimization variables in GALLOP include the following: 1) the impulsive ΔV on each segment, 2) the Julian dates at the launch, flyby, and destination bodies, 3) the launch V_∞ , 4) the incoming inertial velocity vectors at all of the postlaunch bodies, 5) the spacecraft mass at each body, 6) the flyby periapsis altitude at the gravity-assist bodies, and 7) the B-plane angle at the gravity-assist bodies. The optimization program can alter these variables to find feasible and optimal solutions of the given problem. A feasible solution means that the variables satisfy the constraints. These constraints include upper bounds on the impulsive ΔV on each of the segments, the launch- V_∞ magnitude, and the encounter dates at the bodies. Within the feasible set of solutions, the optimizer can find a solution which maximizes the final mass of the spacecraft.

We have the choice to parameterize the encounter velocities in either cartesian or spherical coordinates (a choice we did not have when we attempted to design a low- V_∞ Aldrin cycler in 2002, when GALLOP, in its early stages of development, could only represent the V_∞ in cartesian coordinates¹⁵). If the coordinate system used is spherical, then GALLOP allows constraints on the magnitude, cone, and clock angles of the V_∞ vector. To reduce the V_∞ , we constrain the magnitude of the vectors (and leave the angles unconstrained) for each optimization run (while maximizing final spacecraft mass). We then gradually lower the upper bounds on the V_∞ magnitudes and re-optimize the result using the previous run as an initial guess.

The Aldrin cycler theoretically repeats forever because the positions of the spacecraft, Earth, and Mars in inertial space repeat every 14.95 years (seven Earth-Mars synodic periods). Therefore, to ensure that our modified Aldrin cycler retains its repeatability, we must constraint the total time-of-flight to 14.95 years. As we gradually lower the upper bounds on the V_∞ magnitudes, the (unconstrained) encounter dates also change, in part to accommodate the changing orbit shape. (Our experience is that Mars encounter dates typically move forward when Mars V_∞ are lowered.) As we progressively decrease the V_∞ upper bounds, the Mars flyby dates increasingly move forward in time; eventually we reach a point where further tightening of the V_∞ constraints results in a non-convergent optimization run. (When this happens, the typical run time increases from approximately 10 minutes to several hours on our Sun Blade 1000 workstation equipped with 1 gigabyte of memory.) We note that all of our resulting trajectories still have coasting arcs, suggesting that the V_∞ could be lower, because the vehicle has not exhausted all of its opportunity to thrust. The cases we present in this paper are thus suboptimal in terms of the lowest achievable V_∞ magnitudes, but are optimal in terms of final spacecraft mass (for the particular set of V_∞ constraints). Our main concern here is to show an improvement over previous designs.

Our cycler spacecraft is partially based on the vehicle design in Nock's studies.⁹⁻¹⁰ However, we choose to employ nuclear electric propulsion (NEP) on our cycler vehicle instead of solar electric propulsion (SEP), which was assumed in Nock's work. Our vehicle has the same thrust level as Nock's, but with higher specific impulse (I_{sp}). We assume that our cycler vehicle has a dry mass of 50 metric tons (mt), with up to 25 mt of propellant. The cycler vehicle specifications are summarized in Table 1.

Table 1. Cyclor Vehicle Specifications

Gross Mass	75 mt
Dry Mass	50 mt
Thrust Level	4.12 N
Specific Impulse	6,000 s

The taxi model from Nock is used to calculate the propellant savings that result from V_∞ reductions. An exponential curve-fit is used on the propellant vs V_∞ data from Nock to provide the following equation that calculates the propellant (M_{prop} , in kg) required for the taxi to rendezvous with the cyclor vehicle (for a given V_∞ in km/s) at Mars.

$$M_{\text{prop}} = 7281 \exp(0.275 V_\infty) \quad (1)$$

The taxis are either two- or three- stage rockets, depending on the V_∞ value. For V_∞ less than 7.6 km/s, two-stage taxis are used. For V_∞ that are more than 7.6 km/s, three-stage taxis are required. A curve-fit similar to the one for taxi propellant is used for the taxi stages masses, which include the necessary augmentation tanks and expendable engines. The relationship between hardware mass (M_{hard} , in kg) and V_∞ (in km/s) is described by the following equation.

$$M_{\text{hard}} = 451.77 \exp(0.344 V_\infty) \quad (2)$$

To put the taxi propellant savings into a mission-design perspective, we convert the total propellant requirement (taxi and cyclor vehicle combined) into the required injected mass to a low-Earth orbit (IMLEO). The IMLEO represents the propellant that must be launched from Earth to Mars (in the case of taxi propellant and propellant-related hardware) and from Earth to the cyclor vehicle (to replenish its propellant reserve) every 15 synodic period to maintain the cyclor transportation architecture. We calculate the IMLEO with the rocket equation,¹⁸ based on the following assumptions.

1. Taxi propellant and propellant-related hardware are sent to Mars via a low-energy orbit. This transfer is assumed to have completed in advance of the start of the cyclor trajectory. The total ΔV (the sum of Earth escape, trans-Mars injection, and direct Mars entry) is 7.1 km/s.
2. Cyclor propellant is sent directly to the cyclor vehicle from the low-Earth orbit. The total ΔV is about 4.7 km/s to rendezvous with the cyclor.
3. The ratio of the inert mass to the propellant mass (for all ΔV) for is 16%.
4. The specific impulse (for all ΔV , except the cyclor's) is 450 seconds. We recall from Table 1 that the cyclor has a specific impulse of 6,000 seconds.
5. All ΔV (except the cyclor's) are impulsive.

III. Results

We designed a full 15-year Aldrin cyclor (both inbound and outbound) with V_∞ that are (on the average) lower than the original unmodified Aldrin cyclor.

A. Modified Inbound Aldrin Cyclor (using Low Acceleration)

Table 2 shows the trajectory itinerary of an inbound cyclor with V_∞ constraints. The initial acceleration (a_0 , in m/s^2) of the thruster is

$$a_0 = 5.5 \times 10^{-5} \quad (3)$$

The first column lists the encounters with Earth and Mars and the sequence in the trajectory (for instance, E-1 is the first planetary encounter in the optimized trajectory, and the encounter is with Earth). The second column lists the encounter dates, and the last column shows the encounter velocities. For the inbound cypher, the Mars V_∞ are of particular interest, as the required taxi propellant (and propellant-related hardware mass) to perform hyperbolic rendezvous with the cypher vehicle for each Mars flyby is strongly dependent upon the V_∞ , as shown by Eqs. (1) and (2). The final spacecraft mass (we recall the initial mass is 75 mt) on this inbound cypher trajectory is about 65 mt. In contrast, the unmodified Aldrin cypher needs only 1 mt of propellant.

Table 2. Itinerary of an Inbound Cypher (with V_∞ constraints) using Low Acceleration

Body	Date (mm/dd/yyyy)	V_∞ (km/s)	Unconstrained V_∞^b (km/s)
E-1	5/22/2010	5.513	
M-2	12/11/2011	6.700 ^a	9.025
E-3	6/25/2012	4.945	
M-4	1/22/2014	6.000 ^a	7.710
E-5	8/4/2014	5.236	
M-6	4/6/2016	6.200 ^a	7.216
E-7	9/15/2016	5.630	
M-8	7/10/2018	6.600 ^a	6.808
E-9	12/8/2018	6.471	
M-10	8/20/2020	6.300 ^a	9.704
E-11	2/18/2021	5.141	
M-12	10/13/2022	8.200 ^a	11.903
E-13	3/30/2023	4.354	
M-14	11/19/2024	8.200 ^a	11.035
E-15	6/11/2025	5.612	

^a V_∞ are on upper bound constraints.

^bFrom Ref. 9 and 10; encounters occur on different dates.

As seen in Table 2, all of the Mars V_∞ are at their respective upper bounds. These upper bounds were obtained by a somewhat arbitrary process; they simply represent the lowest V_∞ we could obtain before the optimizer failed to converge. We started our V_∞ -constraining process by selecting the encounters with the highest V_∞ values^{9, 10} (M-2, M-10, M-12, and M-14) shown in the last column of Table 2, and worked our way down until “all the tent poles were pounded into the mud.” It is natural to conclude that our resulting cypher trajectory is not unique, and depends on the order in which we decreased the seven Mars V_∞ . (This process of constraining V_∞ and re-optimizing is a challenging optimization problem on its own right and is not addressed in this paper.)

Due to the complexity of the Aldrin cypher, a trajectory plot (which tends to be “busy”) is not the best way to visualize the orbits. Instead, we show a “radial distance plot,” which illustrates the radial distances (from the Sun) of the spacecraft and the two planets. Encounters are denoted by solid dots on the plot. Figure 1 shows the radial distance plot of the optimized inbound cypher.

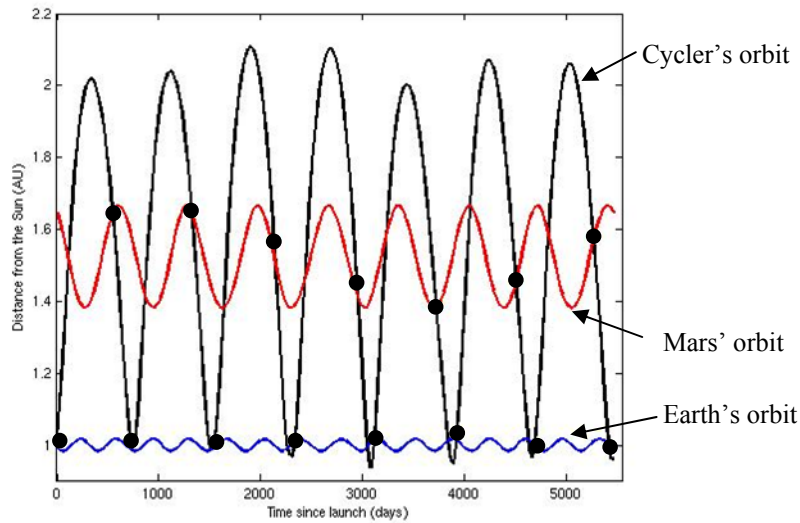


Figure 1. Radial distance plot of the V_{∞} -constrained inbound cyler.

Three curves are shown in Fig. 1. The lowest curve represents the orbit of the Earth, and the small-amplitude oscillation is due to the Earth's (comparatively) small eccentricity. Mars' orbit and the cyler trajectory are similarly represented in the graph. The elapsed time from the beginning to the end of the trajectory in Fig. 1 is roughly 15 years, or 7 Earth-Mars synodic periods. Because the inertial alignments of Earth, Mars, and the cyler vehicle at the beginning and the end (of the interval shown) are nearly the same, the cyler trajectory displayed in Fig. 1 would theoretically extend *ad infinitum* (with very little changes in the trajectory characteristics).

Table 3 shows the same inbound cyler trajectory compared to the unmodified Aldrin cyler (i.e., without V_{∞} constraints). The first three columns are the same as the ones in Table 2; with Earth encounters removed (we only show the Mars encounters because the taxi propellant calculation for the inbound cyler is only dependent on the Mars V_{∞}). The changes in the encounter dates are shown in the fourth column (to demonstrate that the modified trajectory does not deviate too much from the timings of the original Aldrin cyler). Finally, the changes in the V_{∞} and the associated taxi propellant savings are shown in the last two columns of the table.

Table 3. Comparison of with V_{∞} -constrained Trajectory with unmodified Aldrin Cyler (Inbound Cyler)

Encounter	Date (mm/dd/yyyy)	V_{∞} (km/s)	Δ Date (days)	ΔV_{∞} (km/s)	Taxi Propellant Savings (mt)
M-2	12/11/2011	6.700	-28	-2.325	49
M-4	1/22/2014	6.000	-24	-1.710	27
M-6	4/6/2016	6.200	-13	-1.016	15
M-8	7/10/2018	6.600	-1	-0.208	3
M-10	8/20/2020	6.300	-35	-3.404	76
M-12	10/13/2022	8.200	-27	-3.703	146
M-14	11/19/2024	8.200	-12	-2.835	97
Total Taxi Propellant Savings =					414

In Table 3, we note that 2-stage taxis (instead of 3-stage taxis) can now be used at M-2 and M-10, because their respective V_∞ have been reduced to below 6.7 km/s. Even though we were unable to decrease the V_∞ at M-12 and M-14 to lower than 8.2 km/s, the reductions in V_∞ (3.7 km/s and 2.8 km/s, respectively) still result in very large decreases in taxi propellant requirement. We recall that the inbound cycler shown above needs about 10 mt of cycler propellant, while only 1 mt of cycler propellant is required by the unmodified outbound Aldrin cycler. However, we also note the dramatic reduction in the total taxi propellant (414 mt off of the 703 mt required by the unmodified inbound Aldrin cycler) with these V_∞ constraints. Overall, we consider this a favorable propellant trade. Table 4 lists the total IMLEO for these two versions of the inbound Aldrin cycler, we note that even though the cycler propellant expenditure increased ten-fold, the (approximately) 50% reduction in taxi propellant requirement still more than made up for this additional cost.

Table 4. Propellant IMLEO (per 7 synodic periods) Comparison

Trajectory	Taxi Propellant IMLEO (mt)	Cyclor Propellant IMLEO (mt)	Total IMLEO (mt)
Unmodified Aldrin Cyclor	13,355	4	13,359
Aldrin Cyclor with Reduced V_∞	6,486	39	6,525

Figure 2 shows the comparison of the radial distance curves of the V_∞ -constrained trajectory (solid curve) and that of the unmodified Aldrin cycler (dashed curve).

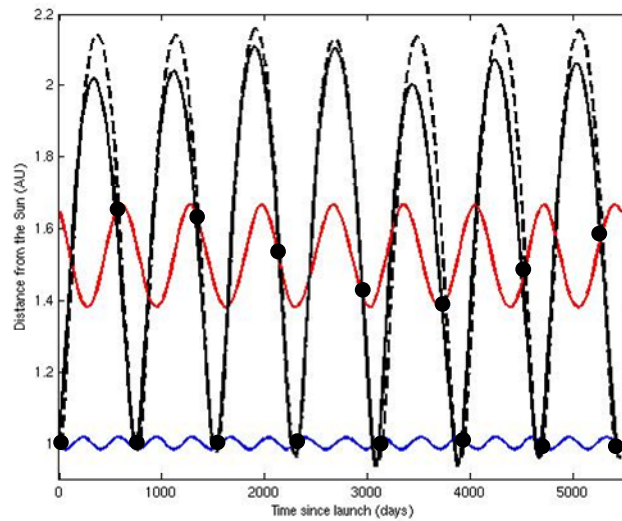


Figure 2. Comparison of radial distance curves.

In Fig. 2 we note the significant reduction in the “overshoot” of the cycler curve at just prior to all Mars encounters (these reductions would not be easily seen on a trajectory plot), especially at M-2, M-4, M-10, M-12, and M-14 (where the largest V_∞ decreases occur). These reductions in the overshoot decrease the angles between the cycler’s and Mars’ velocity vectors at encounters, thus resulting in lower V_∞ . (Actually, the changes in encounter dates also provide some reductions in the V_∞ , but to a lesser extent.) We recall that the inbound cycler shown here does not have the lowest achievable V_∞ values, in part due to the fact that our relatively low thrust level can only modify the orbit shape in a limited way.

B. Modified Inbound Aldrin Cyclor (using High Acceleration)

We now increase the thrust level, doubling it to 8.24 N. The corresponding initial acceleration is

$$a_0 = 1.1 \times 10^{-4} \tag{4}$$

Table 5 shows one such resulting inbound cyclor trajectory.

Table 5. An Inbound Cyclor with High Acceleration^a

Encounter	Date (mm/dd/yyyy)	V_∞ (km/s)	Δ Date (days)	ΔV_∞ (km/s)	Taxi Propellant Savings (mt)
M-2	11/10/2011	5.000	-59	-4.025	69.37
M-4	01/02/2014	5.000	-44	-2.710	37.90
M-6	03/18/2016	5.000	-32	-2.216	28.74
M-8	05/28/2018	5.000	-44	-1.808	22.06
M-10	07/29/2020	5.000	-57	-4.704	90.61
M-12	09/01/2022	5.000	-69	-6.903	194.38
M-14	09/28/2024	5.000	-64	-6.035	145.79
Total Taxi Propellant Savings =					588.86

^aThe initial mass is 75 and the final mass is 55.3 mt. Thrust is 8.24 N, Isp is 6,000 s.

Table 5 shows dramatic reductions in V_∞ values at all Mars encounters (all are below 6.7 km/s, thus two-stage taxis can be used at all Mars encounters). The resulting reduction in taxi propellant is a staggering 589 mt (we recall that for the unmodified inbound Aldrin cyclor, the taxi would need a total of 703 mt of propellant). The resulting total IMLEO for the inbound cyclor shown in Table 5 is only 3,380 mt (a 75% reduction of the IMLEO of the unmodified Aldrin cyclor). Table 6 summarizes the IMLEO values for all the inbound cases considered.

Table 6. Inbound Cyclors Comparison

Trajectory	Taxi Propellant IMLEO (mt)	Cyclor Propellant IMLEO (mt)	Total IMLEO (mt)
Unmodified Aldrin Cyclor	13,355	4	13,359
Aldrin Cyclor with Reduced V_∞ (low acceleration case)	6,486	39	6,525
Aldrin Cyclor with Reduced V_∞ (high acceleration case)	3,300	80	3,380

C. Modified Outbound Aldrin Cyclor (using High Acceleration)

Though not as crucial as in the inbound cyclor, the Mars encounter V_∞ for the outbound case should be low as well. Low speed at Mars arrival increases the (width of the) entry corridor for the atmospheric entry, reduces the structural mass of the Mars taxi, and reduces the g-acceleration load on the crew. In the original outbound Aldrin cyclor, the Mars arrival V_∞ is especially high (above 10 km/s) at the M-2, M-4, and M-6 encounters.

Using the same techniques described for the inbound cyclor, we now bring these V_∞ down to 9.0 km/s. In this process, the spacecraft final mass is maximized while all Earth and Mars encounter dates are

allowed to move freely. The total time of flight is constrained to 15 years. Figure 3 shows the radial distance plot of an outbound cycler with V_∞ constrained. Though not shown in the figure, there are similar reductions in the overshoot as in the case of the inbound cycler.

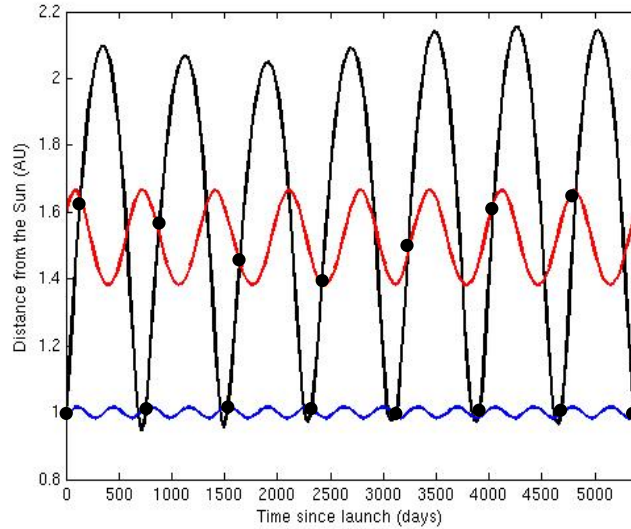


Figure 3. Radial distance plot of the V_∞ -constrained outbound cycler.

In this case we pick our cycler vehicle to be a scaled-up version of the Jupiter Icy Moons¹⁹ (JIMO) spacecraft with a specific impulse of 6,000 s, so that

$$a_0 = 1.1 \times 10^{-4} \quad (5)$$

From the optimization of the entire seven consecutive missions, in which every Mars flyby V_∞ is at or less than 9.0 km/s (compared to up to 11.5 km/s in the original Aldrin Cycler), we find that the final mass at E15 is 91.42% of the initial mass at E1. This propellant requirement for the interplanetary vehicle is modest, considering that the JIMO spacecraft for the Jupiter mission consumes twice the propellant in half the duration. Table 7 shows the difference between the unmodified outbound cycler and the V_∞ -constrained cycler.

Table 7. Comparison of V_∞ -constrained Trajectory (with high acceleration) to unmodified Aldrin Cycler (Outbound Cycler)

Encounter	Date (mm/dd/yyyy)	V_∞ (km/s)	Δ Date (days)	ΔV_∞ (km/s)
M-2	5/14/2012	9.000	20	-1.142
M-4	6/2/2014	9.000	15	-2.449
M-6	7/5/2016	9.000	19	-2.488
M-8	8/19/2018	8.325	10	-0.589
M-10	10/31/2020	7.193	-10	1.428
M-12	1/21/2023	7.065	-3	1.234
M-14	3/16/2025	7.935	2	1.974

We note that in Table 7, several Mars encounters have their respective V_∞ lowered, while the others show increased V_∞ values. However, the main issue here is to bring down the most extreme V_∞ (M-2, M-4, and M-6) from nearly 12 km/s to a more manageable 9 km/s.

An optimal low-thrust trajectory is uniquely determined by the initial acceleration (a_0) and specific impulse (I_{sp}). Thus the propellant mass fraction is the same for a human vehicle of any size scaled from the robotic JIMO spacecraft, as long as these two parameters are the same. In our case, for instance, the propellant is about 10% of the initial mass. Let us now assume that 40% of the initial mass is accounted for as hardware mass that includes reactor, radiator, structure, propulsion systems, and propellant tank, leaving the remaining 50% of the initial mass for the payload. In other words, if a 20-mt JIMO spacecraft were flown in our outbound Aldrin cyclers, the vehicle can carry 10 mt of payload. For a spacecraft five times the size of JIMO, the payload mass is 50 mt, a reasonable value for a human mission. (For example, in NASA's Design Reference Mission,²⁰ the interplanetary Earth Return Vehicle has a payload mass of 27 mt; this payload mass includes crew cabin, life support system, consumables, etc., for six astronauts for an interplanetary flight of six months.) If ten times the size of JIMO is assumed—now requiring an electric power of 1 megawatt—the payload mass is 100 mt, making the interplanetary vehicle a comfortable haven for a large number of Mars explorers.

Of course, the payload capability will improve (percentage-wise) for a larger vehicle; a megawatt-class NEP vehicle will enjoy the lower specific mass (in kg/kW) of a large nuclear reactor and will probably employ thrusters with high thrust density. The selections of a_0 and I_{sp} for the cycler vehicle, however, will involve a complicated interplay between the trajectory and hardware designs of the cycler vehicle, Earth taxi, and the Mars taxi.

IV. Conclusion

With low-thrust propulsion, we mollify one of the biggest drawbacks of the Aldrin cycler—its high V_∞ values at Mars. We present several attractive trajectories with significantly reduced encounter velocities, and consequently, reduced total IMLEO. Even though the initial costs to get the cycler architecture going are not considered in this paper, our analyses show that the cost to sustain such a system (once it is up and running), can be dramatically reduced by decreasing the V_∞ .

References

- ¹Walberg, G., "How Shall We Go to Mars? A Review of Mission Scenarios," *Journal of Spacecraft and Rockets*, Vol. 30, No. 2, April 1993, pp. 129-139.
- ²Hollister, W. M., "Castles in Space," *Astronautica Acta*, Vol. 14, 1969, pp. 311-316.
- ³Rall, C. S. and Hollister, W. M., "Free-Fall Periodic Orbits Connecting Earth and Mars," AIAA Paper No 71-92, AIAA 9th Aerospace Sciences Meeting, New York, NY, Jan. 25-27, 1971.
- ⁴Friedlander, A. L., Niehoff, J. C., Byrnes, D. V., and Longuski, J. M., "Circulating Transportation Orbits Between Earth and Mars," AIAA Paper 86-2009, AIAA/AAS Astrodynamics Conference, Williamsburg, VA, Aug. 18-20, 1986.
- ⁵Aldrin, B., "Cyclic Trajectory Concepts," SAIC presentation to the Interplanetary Rapid Transit Study Meeting, Jet Propulsion Laboratory, Oct. 28, 1985.
- ⁶Byrnes, D. V., Longuski, J. M., and Aldrin, B., "Cycler Orbit Between Earth and Mars," *Journal of Spacecraft and Rockets*, Vol. 30, No. 3, May-June 1993, pp. 334-336.
- ⁷McConaghy, T. Troy, Longuski, James M., and Byrnes, Dennis V., "Analysis of a Class of Earth-Mars Cycler Trajectories," *Journal of Spacecraft and Rockets*, Vol. 41, No. 4, July-August 2004, pp. 622-628.
- ⁸Byrnes, Dennis V., McConaghy, T. Troy, and Longuski, James M., "Analysis of Various Two Synodic Period Earth-Mars Cycler Trajectories," AIAA/AAS Astrodynamics Specialist Conference, AIAA Paper 2002-4423, Monterey, CA, August 2002.
- ⁹Nock, K. T., "Cyclical Visits to Mars via Astronaut Hotels," Phase I Final Report, NASA Institute for Advanced Concepts, Universities Space Research Association Research Grant 07600-049, Nov. 30, 2000. The report can be downloaded from http://www.niac.usra.edu/files/studies/final_report/454Nock.pdf.
- ¹⁰Nock, K. T., "Cyclical Visits to Mars via Astronaut Hotels," Phase II Final Report, NASA Institute for Advanced Concepts, Universities Space Research Association Research Grant 07600-059, April 9, 2003. The report can be downloaded from http://www.niac.usra.edu/files/studies/final_report/524Nock.pdf.

¹¹Landau, D. F. and Longuski, J. M., "Guidance Strategy for Hyperbolic Rendezvous," AIAA Paper 2006-6299, *accepted (March 2006) for presentation at the AIAA/AAS Astrodynamics Specialist Conference*, Keystone, CO, August 21–26, 2006.

¹²Sims, J. A. and Flanagan, S. N., "Preliminary Design of Low-Thrust Interplanetary Missions," AAS Paper 99-338, AAS/AIAA Astrodynamics Specialist Conference, Girdwood, AK, Aug. 16-19, 1999.

¹³McConaghy, T. T., Ph.D. Thesis, School of Aeronautics and Astronautics, Purdue University, West Lafayette, Feb 2004.

¹⁴McConaghy, T. T., Debban, T. J., Petropoulos, A. E., and Longuski, J. M., "Design and Optimization of Low-Thrust Trajectories with Gravity Assists," *Journal of Spacecraft and Rockets*, Vol. 40, No. 3, May-June 2003, pp. 380-387.

¹⁵Chen, Joseph K., McConaghy, T. Troy, Okutsu, Masataka, and Longuski, James M., "A Low-Thrust Version of the Aldrin Cypher," AIAA/AAS Astrodynamics Specialist Conference, AIAA Paper 2002-4421, Monterey, CA, August 2002.

¹⁶Chen, K. J., Landau, D. F., McConaghy, T. T., Okutsu, M., Longuski, J. M., and Aldrin, B., "Powered Earth-Mars Cypher with Three-Synodic-Period Repeat Time," *Journal of Spacecraft and Rockets* Vol. 42, no. 5, 2005, pp. 921-927.

¹⁷Gill, P. E., Murray, W., and Saunders, M. A., "SNOPT: An SQP algorithm for large-scale constrained optimization," *SIAM Journal on Optimization*, Vol. 12, 2002, pp. 979-1006.

¹⁸Landau, D. F. and Longuski, J. M., "Comparative Assessment of Human-Mars-Mission Technologies and Architectures," Purdue University, School of Aeronautics & Astronautics, West Lafayette, IN, July 2006.

¹⁹Yam, C. H., McConaghy, T. T., Chen, K. J., and Longuski, J. M., "Preliminary Design of Nuclear Electric Propulsion Missions to Outer Planets," AIAA/AAS Astrodynamics Specialist Conference, AIAA Paper 2004-5393, Providence, RI, Aug. 16-19, 2004.

²⁰Drake, B. G., ed., "Reference Mission Version 3.0 Addendum to the Human Exploration of Mars: The Reference Mission of the NASA Mars Exploration Study Team," EX-98-036, Houston, TX, June 1998.